Quark Transversity Distributions in the Nucleon using the LaMET approach

Lisa Walter (Regensburg University), Fei Yao (Bejing Normal University),

Jiunn-Wei Chen, Jun Hua, Xiangdong Ji, Luchang Jin, Sebastian Lahrtz, Lingquan Ma, Protick Mohanta, Andreas Schäfer, Hai-Tao Shu, Yushan Su, Peng Sun, Xiaonu Xiong, Yi-Bo Yang, Jian-Hui Zhang

39th International Symposium on Lattice Field Theory, Bonn

08/10/2022

Transversity parton distribution function

- Parton distribution functions (PDFs) [1] are crucial inputs for interpreting experimental data collected at high-energy colliders such as the EIC

- Transversity PDF describes correlation between the transverse polarization of the nucleon and its quark constituents → important for describing the spin structure of the nucleon [2]

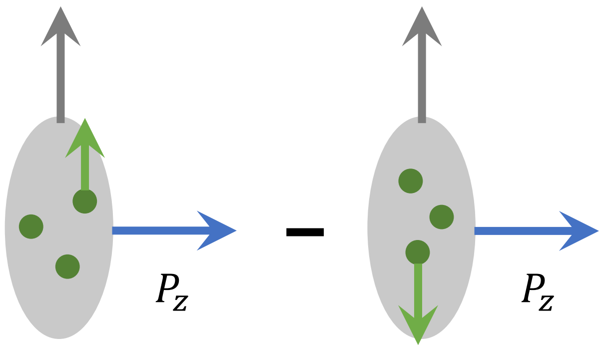

- Less constrained from experiments compared to helicity or unpolarized PDF because it is chiral odd → coupling to other chiral-odd quantities to be measured in experiments [3-5] (spin-asymmetries in e.g. SIDIS or Drell-Yan [6,7])

- Recent theoretical developments [8-13] made lattice QCD calculation of x-dependence of transversity PDF [14-16] possible → several calculations using LaMET [9-10,17] or the pseudo-PDF [13] approach

- Purpose of this work: reliable prediction for isovector quark transversity PDF of the proton (using LaMET) that uses proper renormalization and is valid in continuum and physical mass limit

1: J. P. Ralston and D. E. Soper, Nucl. Phys. B **152**, 109 (1979)
2: R. L. Jaffe and X.-D. Ji, Phys. Rev. Lett. **67**, 552 (1991)
3: R. L. Jaffe and X.-D. Ji, Nucl. Phys. **B375**, 527 (1992)
4: J. L. Cortes et al., Z. Phys. C **55**, 409 (1992)
5: R. L. Jaffe and X.-D. Ji, hep-ph/9307329
6: M. Constantinou et al., 2006.08636
7: L. Gamberg et al., 2205.00999
8: V. M. Braun et al., 0709.1348
9: X. Ji, 1305.1539
10: X. Ji, 1404.6680
11: Y.-Q. Ma et al., 1709.03018
12: H.-W. Lin et al., 1711.07916
13: A. V. Radyushkin, 1705.01488
14: C. Alexandrou et al., 1807.00232
15: Y.-S. Liu et al., 1810.05043
16: C. Egerer et al., 2111.01808
17: X. Ji et al., 2004.03543

Outline

- Transversity parton distribution function
- CLS ensembles
- Extraction of quasi-LF correlation in LaMET
- Renormalization in hybrid scheme
- Fourier-transformation to momentum space
- Perturbative matching
- Continuum, chiral and infinite momentum extrapolation

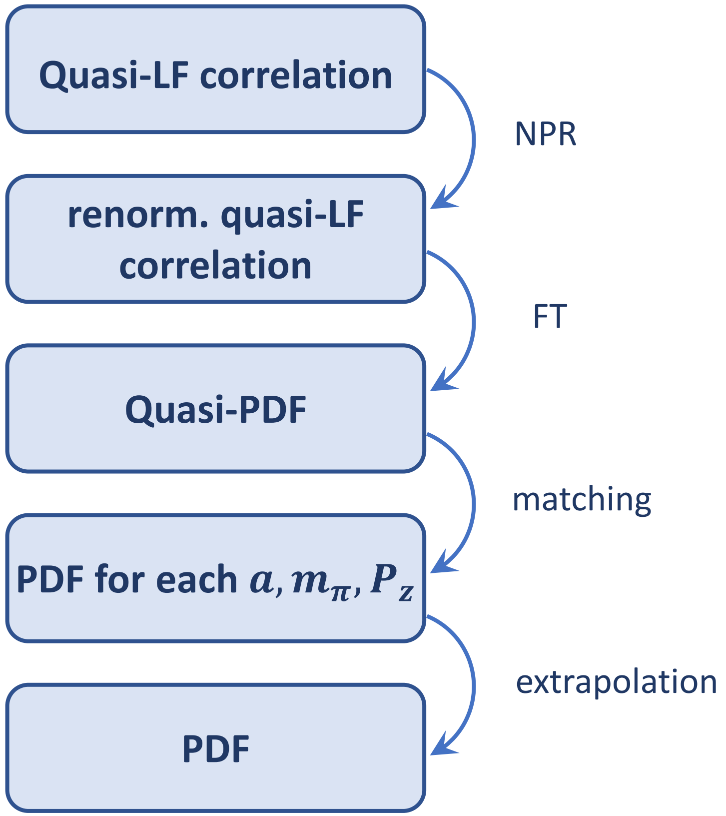

Coordinated Lattice Simulation ensembles [18]

- Lüscher-Weisz gauge action with tree-level coefficients
- Fermions: $O(a)$-improved Wilson Dirac operator
- $N_f = 2 + 1$
- Ensembles with various lattice spacings and pion masses → continuum and chiral extrapolation
- Multiple nucleon momenta P_z on each ensemble → infinite momentum extrapolation

Ensemble	a (fm)	$L^3 \times T$	m_π (MeV)	$m_\pi L$	P_z (GeV)
X650	0.098	$48^3 \times 48$	338	8.1	0, 1.84, 2.37, 2.63
H102	0.085	$32^3 \times 96$	354	4.9	0, 1.82, 2.27, 2.73
H105		$32^3 \times 96$	281	3.9	0, 1.82
C101		$48^3 \times 96$	222	4.6	0, 1.82
N203	0.064	$48^3 \times 128$	348	5.4	0, 1.62, 2.02, 2.43, 2.83, 3.24
N302	0.049	$48^3 \times 128$	348	4.2	0, 2.09, 2.62

Table 1: Details of the simulation setup, including lattice spacing a, lattice size $L^3 \times T$, and pion masses [19]. Proton momenta P_z used in lattice determination of quasi-transversity PDF.

18: M. Bruno et al., 1411.3982
19: G. S. Bali et al., in preparation

Extraction of quasi-LF correlation in LaMET

Leading-twist quark transversity PDF of the proton [2]:

$$\delta q(x,\mu) = \int \frac{d\,\xi^-}{4\,\pi}\, e^{ixP^+\xi^-} \langle PS_\perp|\,\bar{\psi}(0)\gamma^+\gamma^\perp\gamma_5\, W[0,\xi^-]\psi(\xi^-)|PS_\perp\rangle$$

$|PS_\perp\rangle$: transversely polarized proton (polarization $S_\perp$) with momentum P along z direction

x: momentum fraction carried by the quark, μ: renormalization scale in the $\overline{\mathrm{MS}}$ scheme

$\xi^\pm = (\xi^t \pm \xi^z)/\sqrt{2}$: light-cone coordinates

$W[0,\xi^-]$: gauge link along the light-cone direction

Transversity quasi-PDF:

$$\delta\tilde{q}(x,\ P_z, 1/a) = N\int \frac{d\,z}{4\,\pi}\, e^{ixzP_z}\, \tilde{h}(z,\, P_z, 1/a)$$

$\boldsymbol{\tilde{h}(z, P_z, 1/a) = \langle PS_\perp|\,\bar{\psi}(z)\gamma^t\gamma^\perp\gamma_5\, W[z,0]\psi(0)|PS_\perp\rangle}$**: equal-time / quasi-light-front correlation**

$\lambda = zP_z$: quasi light-cone distance

→ flavor combination $\delta\tilde{u}(x) - \delta\tilde{d}(x)$ to eliminate disconnected contributions

2: R. L. Jaffe and X.-D. Ji, Phys. Rev. Lett. **67**, 552 (1991)

Extraction of quasi-LF correlation in LaMET

Lattice calculation of two-point and three-point functions

- calculate $C^{2\text{pt}}(P_z, t_{\text{sep}})$ and $C_\Gamma^{3\text{pt}}(P_z, t, t_{\text{sep}})$ on the lattice to extract **ground state matrix element** $\boldsymbol{\tilde{h}(z, P_z, 1/a)}$
- LQCD calculations performed using the Chroma software suite [20] and IDFLS solver [21]
- momentum smearing [22] to improve signal-to-noise ratio of calculations with high-momentum nucleon states

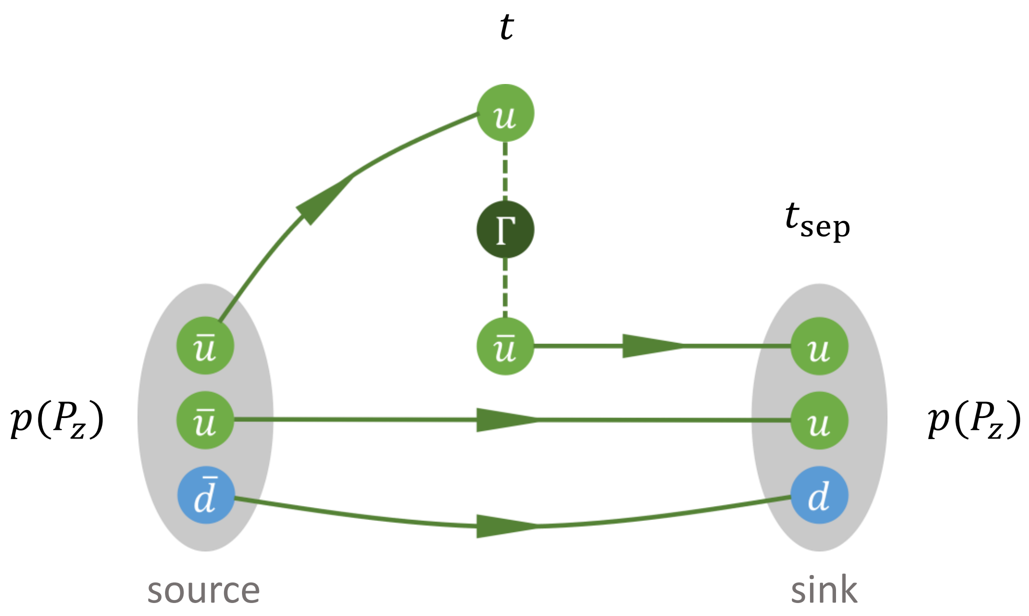

Figure 1: Schematic figure of three-point function. t_{sep}: source-sink separation, t: insertion time.

20: R. G. Edwards et al., hep-lat/0409003
21: M. Lüscher, 0710.5417
22: G. S. Bali et al., 1602.05525

Extraction of quasi-LF correlation in LaMET

- Calculation of multiple source-sink separations for each ensemble

- **Decomposition of correlation functions**

$$C^{2\text{pt}}(P_z, t_{\text{sep}}) = |A_0|^2 e^{-E_0 t_{\text{sep}}} + |A_1|^2 e^{-E_1 t_{\text{sep}}} + \dots$$

$$C_\Gamma^{3\text{pt}}(P_z, t, t_{\text{sep}}) = |A_0|^2 \langle \mathbf{0}|\boldsymbol{O}_\Gamma|\mathbf{0}\rangle\, e^{-E_0 t_{\text{sep}}}$$

$$+|A_1|^2\, \langle 1|O_\Gamma|1\rangle e^{-E_1 t_{\text{sep}}}$$

$$+A_1 A_0^* \langle 1|O_\Gamma|0\rangle e^{-E_1 (t_{\text{sep}}-t)} e^{-E_0 t}$$

$$+A_0 A_1^* \langle 0|O_\Gamma|1\rangle e^{-E_0 (t_{\text{sep}}-t)} e^{-E_1 t} + \dots$$

$\langle \mathbf{0}|\boldsymbol{O}_\Gamma|\mathbf{0}\rangle = \tilde{\boldsymbol{h}}(\boldsymbol{z}, \boldsymbol{P_z}, \mathbf{1}/\boldsymbol{a})$ **: ground state matrix element**

Ensemble	$N_{\text{conf.}}$	t_{sep} / a	$N_{\text{meas.}}$ / $N_{\text{conf.}}$
X650	1000	7, 8, 9	1
H102	500	7, 8, 9	2
H105	500	7, 8, 9	2
C101	500	6, 7, 8, 9	2
N203	500	10, 11, 12, 13, 14, 15	4 8 16
N302	500	10, 12, 14, 16, 18	4 8 16

Table 2: Details of the correlator calculation, including number of configurations $N_{\text{conf.}}$, source-sink separation t_{sep} and number of measurements $N_{\text{meas.}}$ per configuration.

Extraction of quasi-LF correlation in LaMET

Extraction of ground state matrix elements from lattice-calculated correlators by two-state combined fit:

$$C^{2\mathrm{pt}}(t_{\mathrm{sep}}) \approx c_4 e^{-E_0 t_{\mathrm{sep}}}(1 + c_5 e^{-\Delta E t_{\mathrm{sep}}})$$

$$R_\Gamma(z, t, t_{\mathrm{sep}}) \equiv \frac{C^{3\mathrm{pt}}(z, t, t_{\mathrm{sep}})}{C^{2\mathrm{pt}}(t_{\mathrm{sep}})} \approx \frac{\boldsymbol{c_0(z)} + c_1(z)\left[e^{-\Delta E(t_{\mathrm{sep}}-t)} + e^{-\Delta E t}\right] + c_3(z) e^{-\Delta E t}}{1 + c_5 e^{-\Delta E t_{\mathrm{sep}}}}$$

- $\boldsymbol{c_0(z) = \langle 0|O_\Gamma|0\rangle = \tilde{h}(z, P_z, 1/a)}$**: ground state matrix element**
- Neglected contributions beyond ground state and first excited state
- Results from fits with different sets of t_{sep} indicate that excited-state contamination is under control

Extraction of quasi-LF correlation in LaMET

- Good agreement between data and fitting

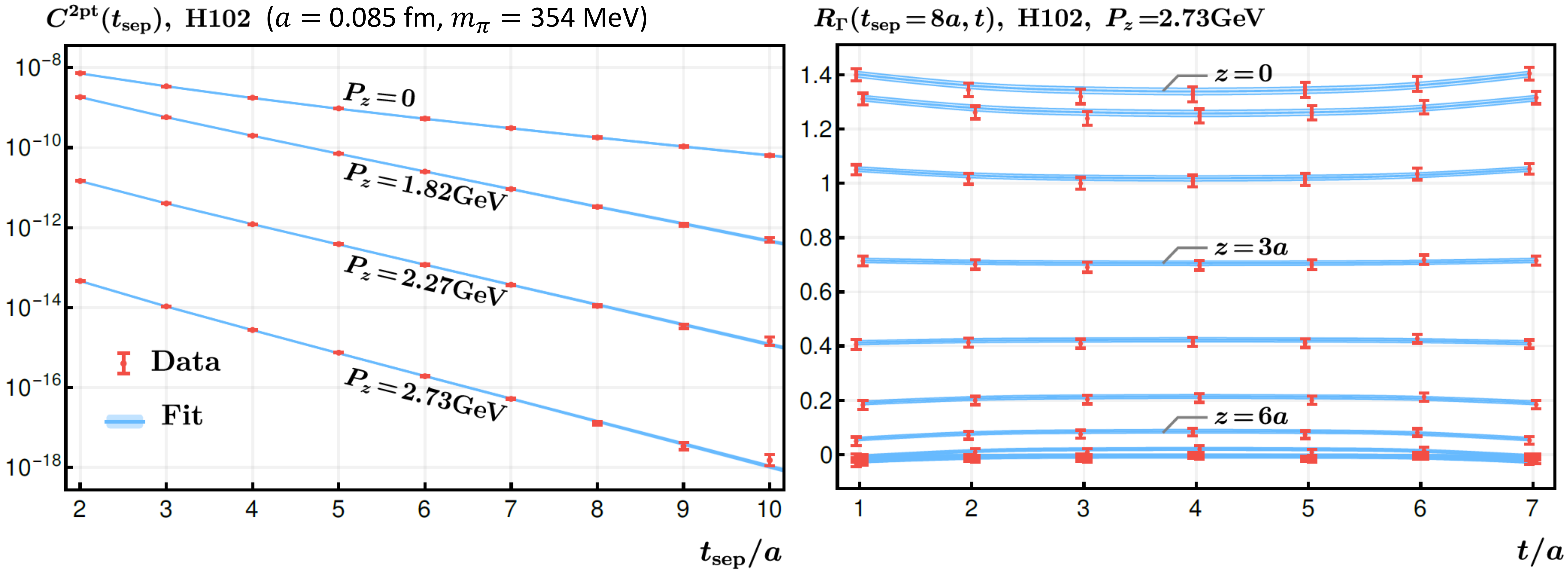

Figure 2: Demonstration of fitting the two-point correlation function $C^{2pt}(t_{sep})$ and the ratio $R_\Gamma(z, t, t_{sep})$ for H102. The data in the R_Γ plot are slightly shifted in $\pm t$ direction for clarity. R_Γ is only shown for $0 \le |z| \le 9$ for demonstration.

Renormalization in hybrid scheme

- Bare quasi-LF correlation contains linear and logarithmic UV divergences → need to be removed by non-perturbative renormalization

- Various approaches suggested and implemented in literature [23-28], but: renormalization distorts IR behaviour [29]

→ **Hybrid scheme [29]: quasi-LF correlations at short and long distances renormalized separately**

$$\tilde{h}_R(z, P_z) = \frac{\tilde{h}(z, P_z, 1/a)}{\tilde{h}(z, P_z = 0, 1/a)} \theta(z_s - |z|) + \eta_s \frac{\tilde{h}(z, P_z, 1/a)}{Z_R(z, 1/a)} \theta(|z| - z_s)$$

- short distances: dividing by matrix element in rest frame (as in ratio scheme [26])
- long distances: self-renormalization [30]: $Z_R(z, 1/a)$ obtained by fitting bare matrix elements at multiple lattice spacings to a perturbative-QCD-dictated functional form
- $z = z_s = 0.3$ fm separates short and long distances
- $\eta_s = Z_R(z_s, 1/a)/\tilde{h}(z_s, P_z = 0, 1/a)$: ensures continuity of renormalized quasi-LF correlation at $z = z_s$

23: J.-W. Chen et al., 1609.08102
24: T. Izubuchi et al., 1801.03917
25: C. Alexandrou et al., 1706.00265
26: A. Radyushkin, 1801.02427
27: V. M. Braun et al., 1810.00048
28: Z.-Y. Li et al., 1809.01836
29: X. Ji et al., 2008.03886
30: Y.-K. Huo et al., 2103.02965

Renormalization in hybrid scheme

- Renormalized quasi-LF correlation for ensembles with nearly same m_π ($\approx 340 - 350$ MeV)
- For all ensembles: Good convergence as P_z increases

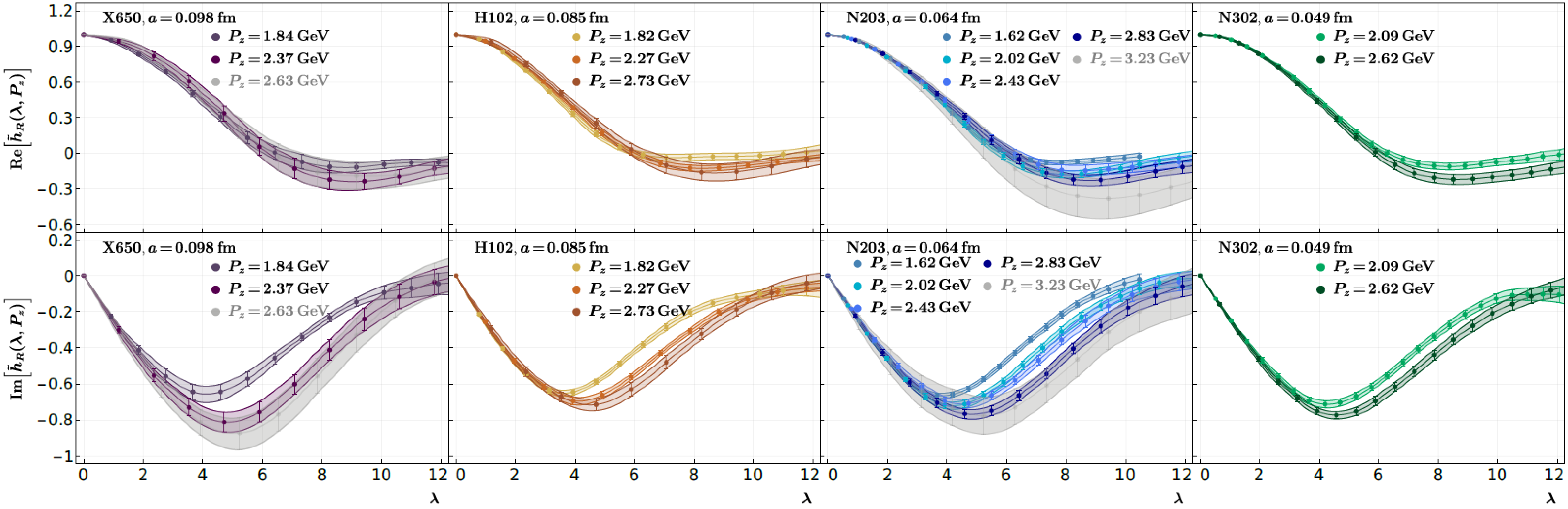

Figure 3: Real (top) and imaginary (bottom) parts of the renormalized matrix elements across different ensembles as functions of $\lambda = zP_z$ at scale μ = 2 GeV.

Renormalization in hybrid scheme

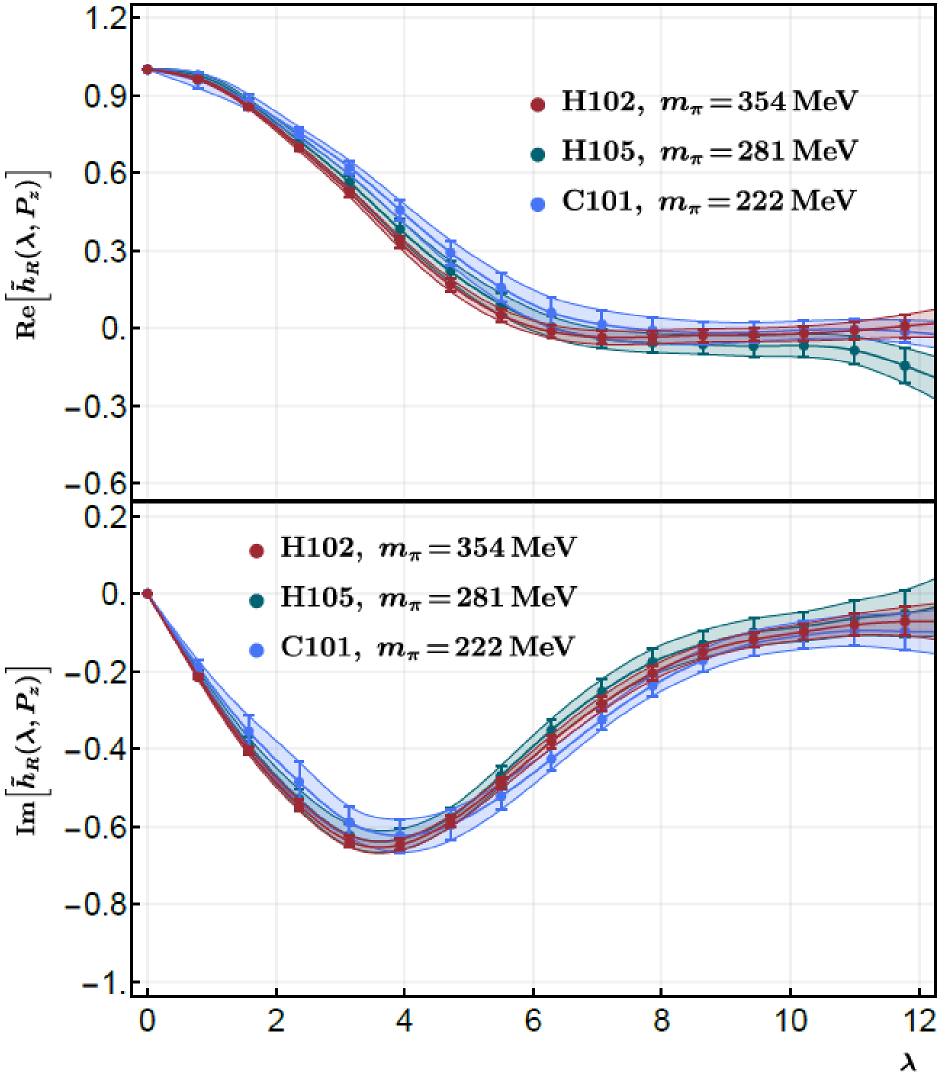

Figure 4: Real (top) and imaginary (bottom) parts of the renormalized matrix elements across different ensembles with a = 0.085 fm and P_z = 1.82 GeV.

- Renormalized quasi-LF correlations on ensembles with same lattice spacing ($a = 0.085$ fm), but different pion masses
- Dependence on m_π only very mild

Fourier-transformation to momentum space

- Quasi-PDF defined as Fourier transform of the quasi-LF correlation
- FT to momentum space requires quasi-LF correlation at all distances z, but uncertainty grows at large z
- Brute-force truncation and FT would lead to unphysical oscillations in momentum space distribution

→ **Physics-based extrapolation form [29] at large quasi-LF distance**

$$H_m^{\mathrm{R}}(z,P_z) = \left[\frac{c_1}{(i\lambda)^a} + e^{-i\lambda}\frac{c_2}{(-i\lambda)^b}\right] e^{-\lambda/\lambda_0}$$

- [...]: power-law behaviour of transversity PDF in endpoint region
- $e^{-\lambda/\lambda_0}$: correlation function has finite correlation length λ_0 at finite momentum

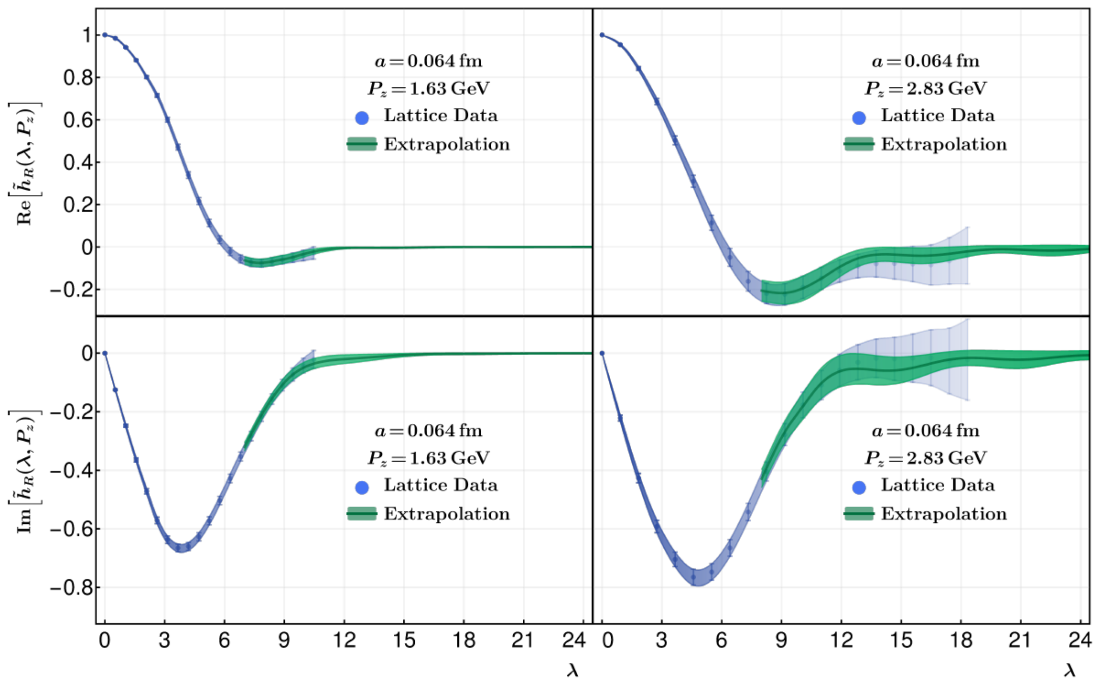

Figure 5: Renormalized matrix elements $\tilde{h}_{\mathrm{R}}(\lambda, P_z)$ for N203 for one small (left) and large (right) momentum with extrapolation to large λ. The extrapolation reproduces the data in moderate λ region and yields smooth correlations in large λ region.

- Details of extrapolation mainly affect final results in region where LaMET expansion breaks down [17]

29: X. Ji et al., 2008.03886
17: X. Ji et al., 2004.03543

Perturbative matching

- Extraction of transversity PDF by perturbative matching (similar calculations in [31, 32])

- **Factorization formula in momentum space:**

$$\delta\tilde{q}(x,P_z) = \int_{-1}^{1}\frac{dy}{|y|}C\left(\frac{x}{y},\frac{\mu}{yP_z}\right)\delta q(y,\mu) + O\left(\frac{\Lambda_{QCD}^2}{(yP_z)^2},\frac{\Lambda_{QCD}^2}{\left((1-y)P_z\right)^2}\right)$$

- One-loop matching kernel in momentum space in hybrid scheme

$$C_h\left(x,\frac{\mu}{p_z},\lambda_s\right) = C_r\left(x,\frac{\mu}{p_z}\right) + \delta C\left(x,\frac{\mu}{p_z},\lambda_s\right) = C_r\left(x,\frac{\mu}{p_z}\right) + \frac{\alpha_s C_F}{\pi}\left[-\frac{1}{|1-x|} + \frac{2\mathrm{Si}\left((1-x)\lambda_s\right)}{\pi(1-x)}\right]_+$$

- Matching kernel in ratio scheme:

$$C_r\left(x,\frac{\mu}{p_z}\right) = \delta(1-x) + \frac{\alpha_s C_F}{2\pi}\begin{cases} \left[\frac{2x}{1-x}\ln\frac{x}{x-1} - \frac{2}{1-x}\right]_+ & x > 1 \\ \left[\frac{2x}{1-x}\left(\ln\frac{4p_z^2}{\mu^2} + \ln x(1-x)\right) + 2\right]_+ & 0 < x < 1 \\ \left[-\frac{2x}{1-x}\ln\frac{x}{x-1} + \frac{2}{1-x}\right]_+ & x < 0 \end{cases}$$

31: V. M. Braun et al., 2108.03065
32: C.-Y. Chou and J.-W. Chen, 2204.08343

Continuum, chiral and infinite momentum extrapolation

- Extracted transversity PDF still contains lattice artifacts
- Calculations not done at infinite momentum
- Calculations not done at $m_\pi = m_{\pi,\text{phys}}$

simultanous extrapolation to continuum, infinite momentum and physical point

- **Functional form including $\boldsymbol{a}, \boldsymbol{P_z}$ and $\boldsymbol{m_\pi}$:**

$$\delta q(x, P_z, a, m_\pi) = \left[\delta q_0(x) + a^2 f(x) + \frac{g(x,a)}{P_z^2}\right]\left(1 + m_\pi^2 k(x)\right)$$

  - $\delta q(x) \equiv \delta q_0(x)\left(1 + m_{\pi,\text{phys}}^2 k(x)\right)$: desired transversity PDF
  - $a^2 f(x)$ term: leading discretization error (coefficient of terms like $a^2 P_z^2$ close to zero)
  - $\frac{g(x,a)}{P_z^2}$ term: leading higher-twist contribution
  - m_π-extrapolation follows from the form used in [33]

33: G. S. Bali et al., 1903.12590

Continuum, chiral and infinite momentum extrapolation

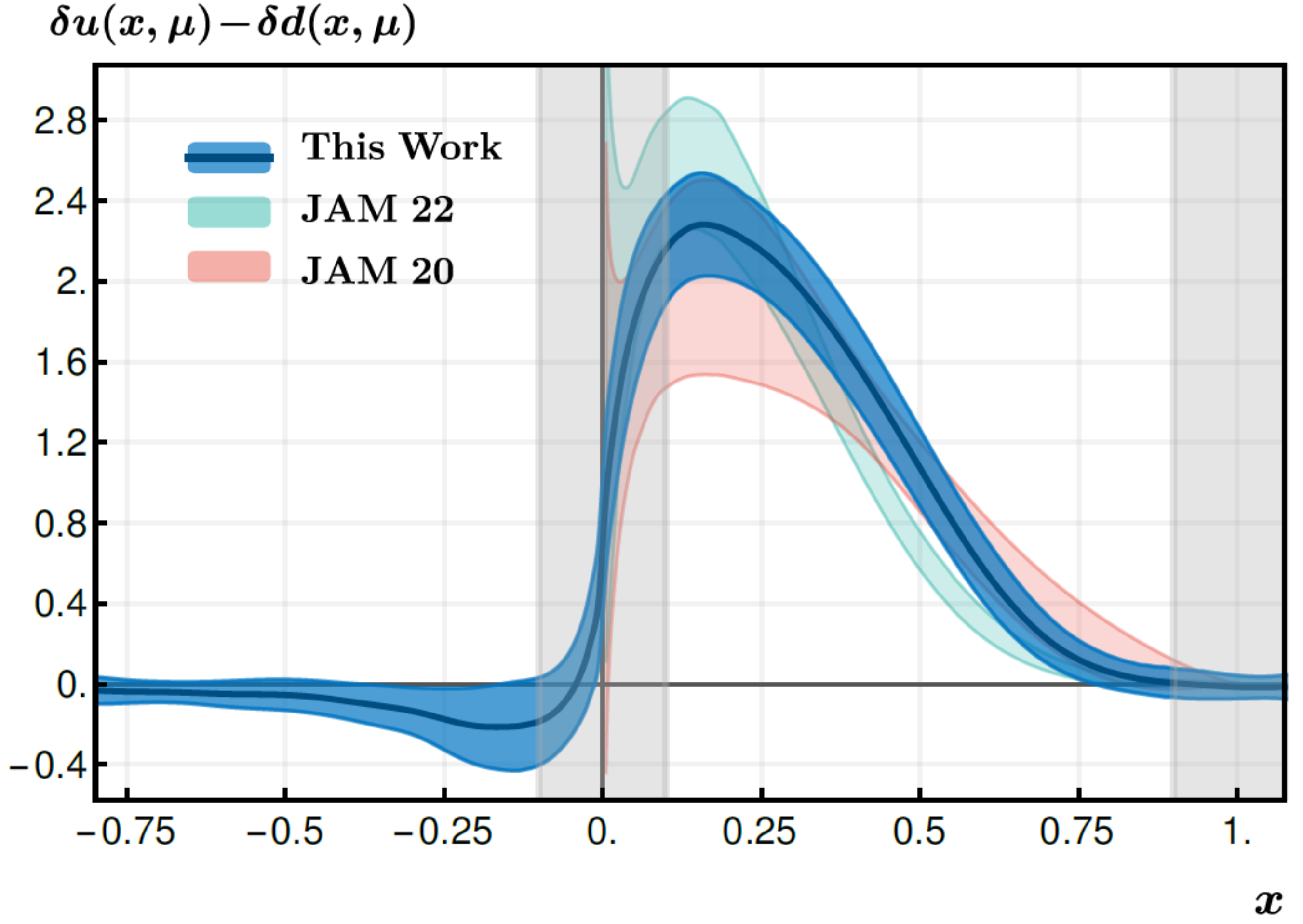

Figure 6: Final proton isovector transversity PDF at renormalization scale μ = 2 GeV, extrapolated to continuum, physical and infinite momentum limit, compared with JAM20 [34] and JAM22 [7] global fits.

- Final result for isovector quark transversity PDF (normalized to g_T) lies between global analyses JAM20 [34] and JAM22 [7]
- For previous lattice QCD calculations of transversity PDF see [14-16]
- Result consistent with zero at negative x
- Grey bands: endpoint regions ($|x| \leq 0.1,\ x \geq 0.9$) where LaMET predictions are not reliable
- Error band includes statistic and systematic uncertainties
  - Renormalization scale dependence
  - Choice of z_s
  - Extrapolation to large λ
  - Combined extrapolation

34: J. Cammarota et al., 2002.08384
7: L. Gamberg et al., 2205.00999
14: C. Alexandrou et al., 1807.00232
15: Y.-S. Liu et al., 1810.05043
16: C. Egerer et al., 2111.01808

Summary and Outlook

Summary:

- Calculation of isovector quark transversity PDF with LaMET at various $a, m_{\pi,} P_z$ with extrapolation to continuum, physical mass and infinite momentum limit
- Multi-state analysis with multiple source-sink separations to remove excited-state contamination
- State-of-the-art renormalization (hybrid scheme) and matching
- Reliable lattice prediction of the isovector quark transversity PDF in the proton → will offer guidance to relevant measurements at JLab and EIC

Outlook:

- Large proton momenta P_z very important for calculations with LaMET → fine lattices crucial
- Possibly analyze even finer lattices, e.g. J501 ($a \approx 0.039$ fm)

Backup slides: Dispersion relation

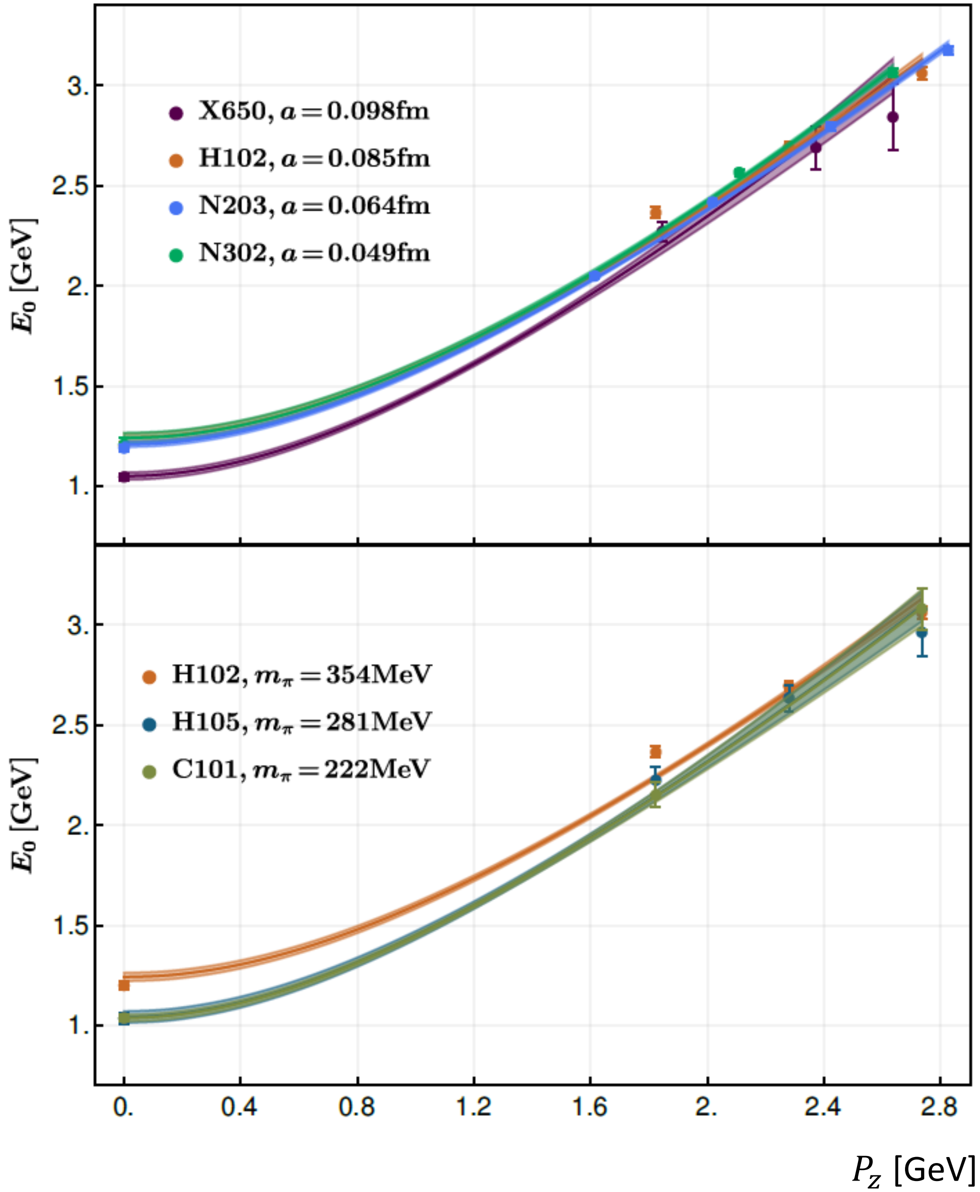

- Effective mass extracted by fitting the two-point correlation function
- Fit effective mass to

$$E(P_z) = \sqrt{m^2 + P_z^2 + c^2 a^2 P_z^4}$$

  - quadratic term in a included to parametrize the discretization error

- Extracted effective masses are consistent with dispersion relation within 3σ error

Figure 7: The dispersion relation of CLS ensembles at four different lattice spacings used in this work. In the upper subfigure we compare ensembles with different lattice spacing but roughly the same π mass: $m_\pi \approx 340$ MeV, while in the lower subfigure we compare ensembles with the same lattice spacing $a \approx 0.085$ fm but different m_π.

Backup slides: Renormalization

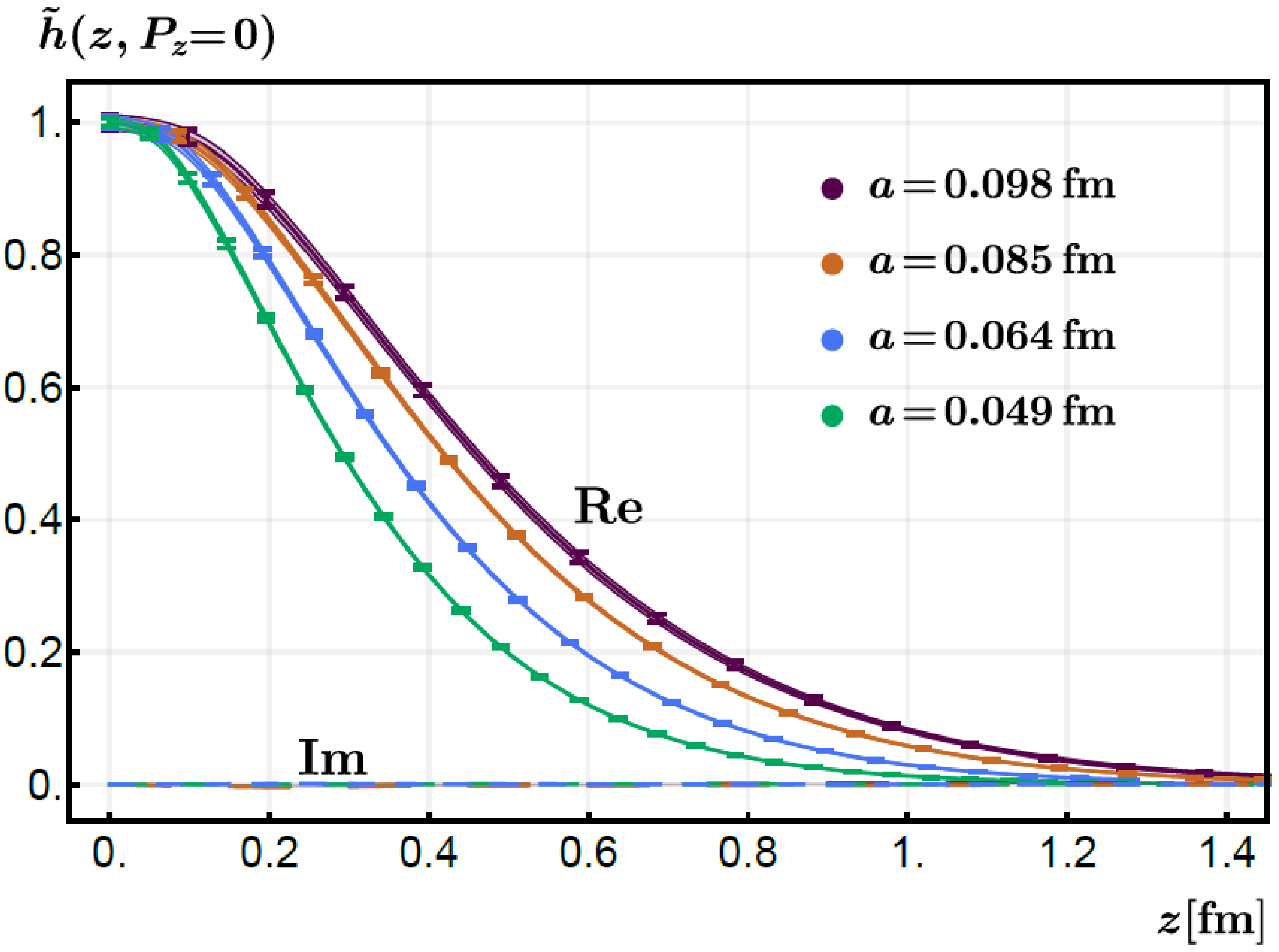

Figure 8: Bare matrix elements in the rest frame. Their imaginary part is consistent with zero.

Short distances: $|z| < z_s$

$$\tilde{h}_R(z, P_z) = \frac{\tilde{h}(z, P_z, 1/a)}{\tilde{h}(z, P_z = 0, 1/a)}$$

- Renormalization factor: inverse of the nucleon matrix element in the rest frame

Backup slides: Renormalization

Long distances: $|\boldsymbol{z}| > \boldsymbol{z_s}$

$$\tilde{h}_R(z, P_z) = \eta_s \frac{\tilde{h}(z, P_z, 1/a)}{Z_R(z, 1/a)}$$

- $\eta_s = Z_R(z_s, 1/a)/\tilde{h}(z_s, P_z = 0, 1/a)$: similar to a scheme conversion factor, guarantees continuity of the renormalized matrix element at $z = z_s$
- Self-renormalization factor $Z_R(z, 1/a)$ is obtained by fitting the bare matrix elements in the rest frame to the following perturbative-QCD-dictated functional form [30]

$$\ln\tilde{h}(z, 1/a) = \frac{kz}{a\ln(a\Lambda_{\mathrm{QCD}})} + \boldsymbol{g(z)} + f(z)a^2 + \frac{3C_F}{11 - 2N_f/3}\ln\left[\frac{\ln[1/(a\Lambda_{\mathrm{QCD}})]}{\ln[\mu/\Lambda_{\mathrm{QCD}}]}\right] + \ln\left[1 + \frac{d}{\ln(a\Lambda_{\mathrm{QCD}})}\right] \quad \textbf{(B1)}$$

  – $\frac{kz}{a\ln(a\Lambda_{\mathrm{QCD}})}$: linear divergence
  – $g(z) = \boldsymbol{g_0(z)} + m_0 z$: nonperturbative physics $g_0(z)$ we are interested in + renormalon ambiguity term
  – $f(z)a^2$: discretization effects
  – Last two terms come from resummation of leading an sub-leading logarithmic divergences
  – Treat d and Λ_{QCD} as fitting parameters to partially account for higher-order pert. effects and remaining lattice artifacts

30: Y.-K. Huo et al., 2103.02965

Backup slides: Renormalization

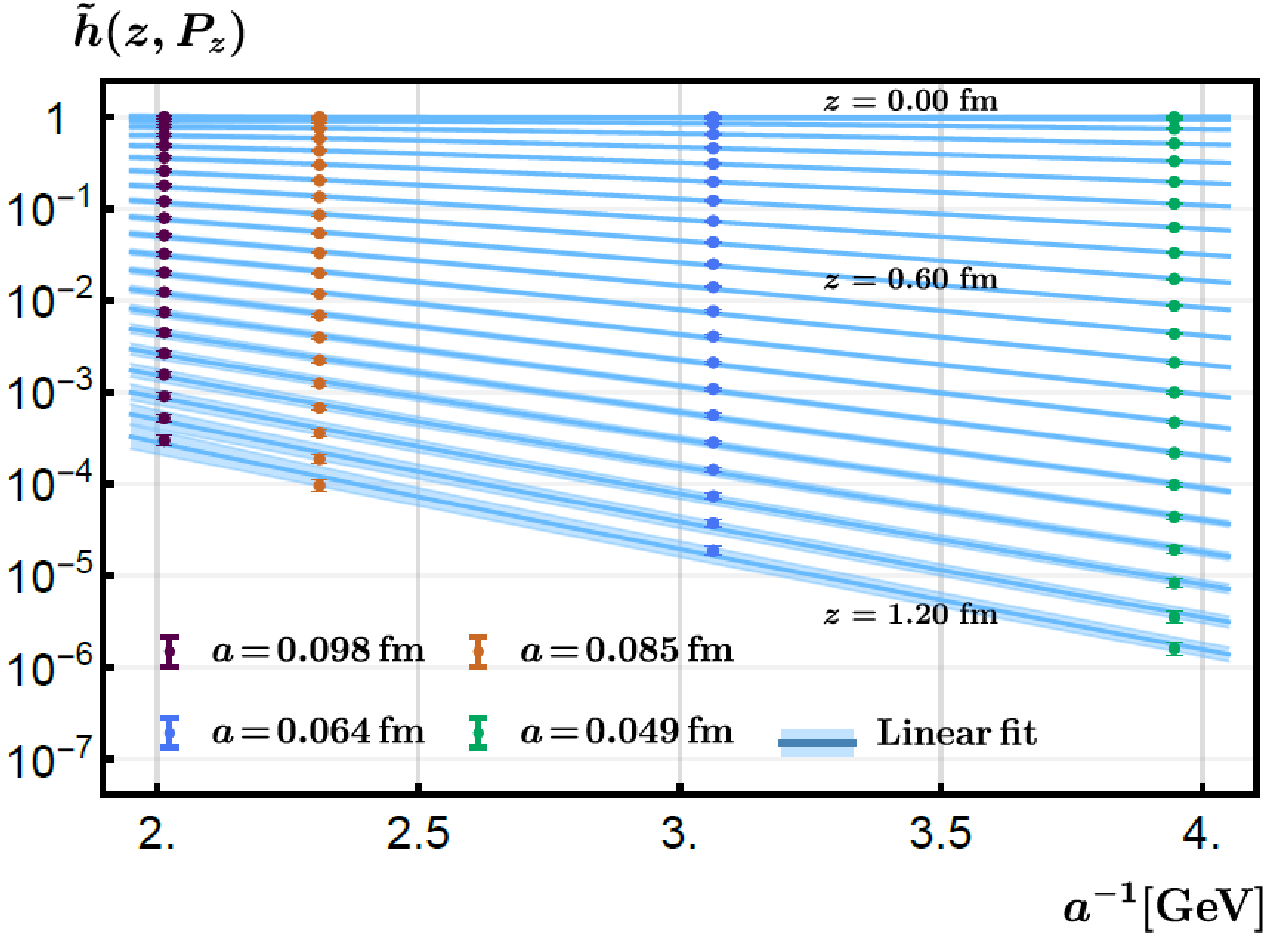

Figure 9: Fit of the bare nucleon transversity matrix elements in the rest frame. Colorful points represent the bare matrix elements from lattice calculation and blue bands are fitted values using eq. (B1). The paramters k and λ_{QCD} are fitted to be $k = 4.356\ \mathrm{GeV}^{-1}\mathrm{fm}^{-1}$ and $\lambda_{\mathrm{QCD}} = 0.1\ \mathrm{GeV}$.

Backup slides: Renormalization

- Renormalization factor given by

$$Z_R(z, 1/a) = \frac{\tilde{h}(z, 1/a)}{\tilde{h}_R(z)}$$

$$\tilde{h}_R(z) = \exp[g(z) - m_0 z] = \exp[g_0(z)]$$

- $\tilde{h}_R(z)$ required to be equal to the continuum perturbative $\overline{\mathrm{MS}}$ result at short distances

$$Z_{\overline{\mathrm{MS}}}(z) = 1 + \frac{\alpha_s C_F}{2\pi}\left(2\ln\left(z^2\mu^2 e^{2\gamma_E}/4\right) + 2\right)$$

(one-loop)

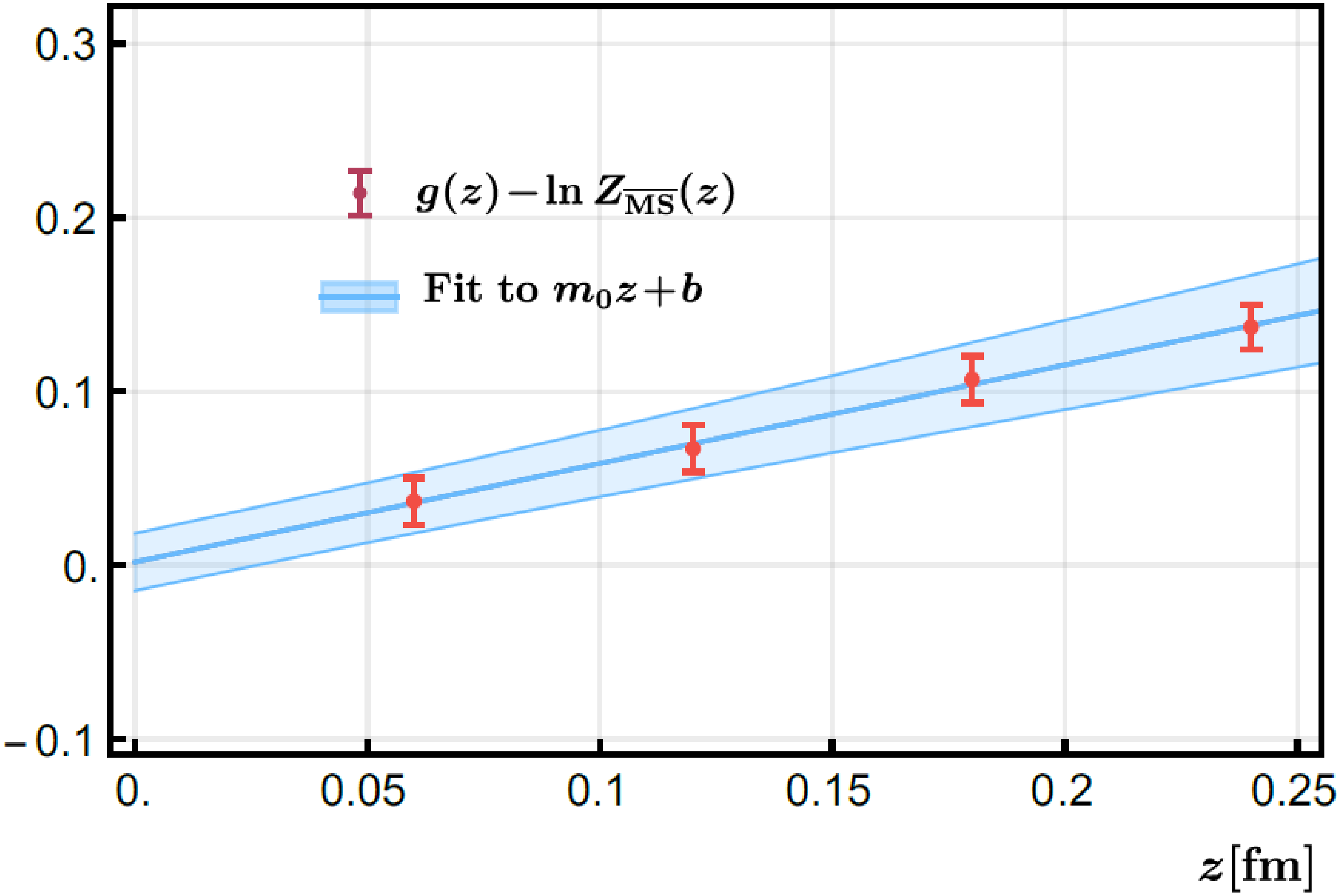

Figure 10: The m_0 fit. Red points are $g(z) - \ln Z_{\overline{\mathrm{MS}}}(z)$ at small-z region. The blue band is the fit to $m_0 z + b$, where we tune the parameter d to minimize $|b|$. The fitting gives $m_0 = 0.57\ \mathrm{fm}^{-1}, d = -0.663$ and $b = 0.00185$.

Backup slides: Renormalization

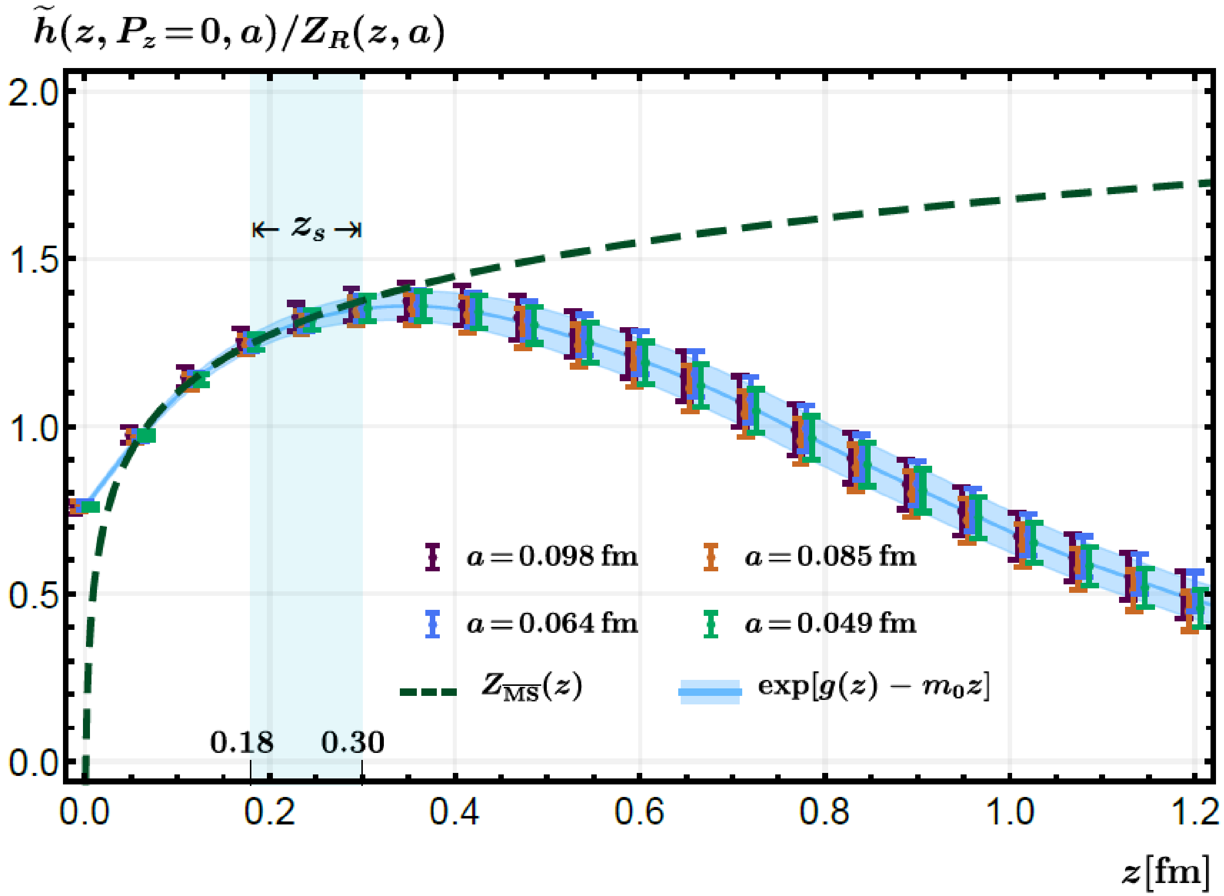

Figure 11: The renormalized matrix element $\tilde{h}(z, P_z = 0, a)/Z_R(z, a, \mu)$ (colorful points) and the fitting renormalized matrix element $\exp[g(z) - m_0 z]$ (blue band) are entirely coincident. We have slightly shifted X650, H102 and N302 data to $\pm x$ direction for clarity. The renormalized matrix elements overlap nicely with the perturbative one-loop result $Z_{\overline{\mathrm{MS}}}(z)$ at short distances, except at very small z where higher-order corrections get important.

Comparison of renormalized matrix element with perturbative one-loop $\overline{\mathbf{MS}}$ result

- Agreement very good at short distances (except at very small z where higher-order corrections get important)
- $z = z_s = 0.3$ fm chosen in analysis
- z_s varied down to 0.18 fm (shaded region) to account for systematic uncertainties related to the choice of z_s

Backup slides: Large λ extrapolation

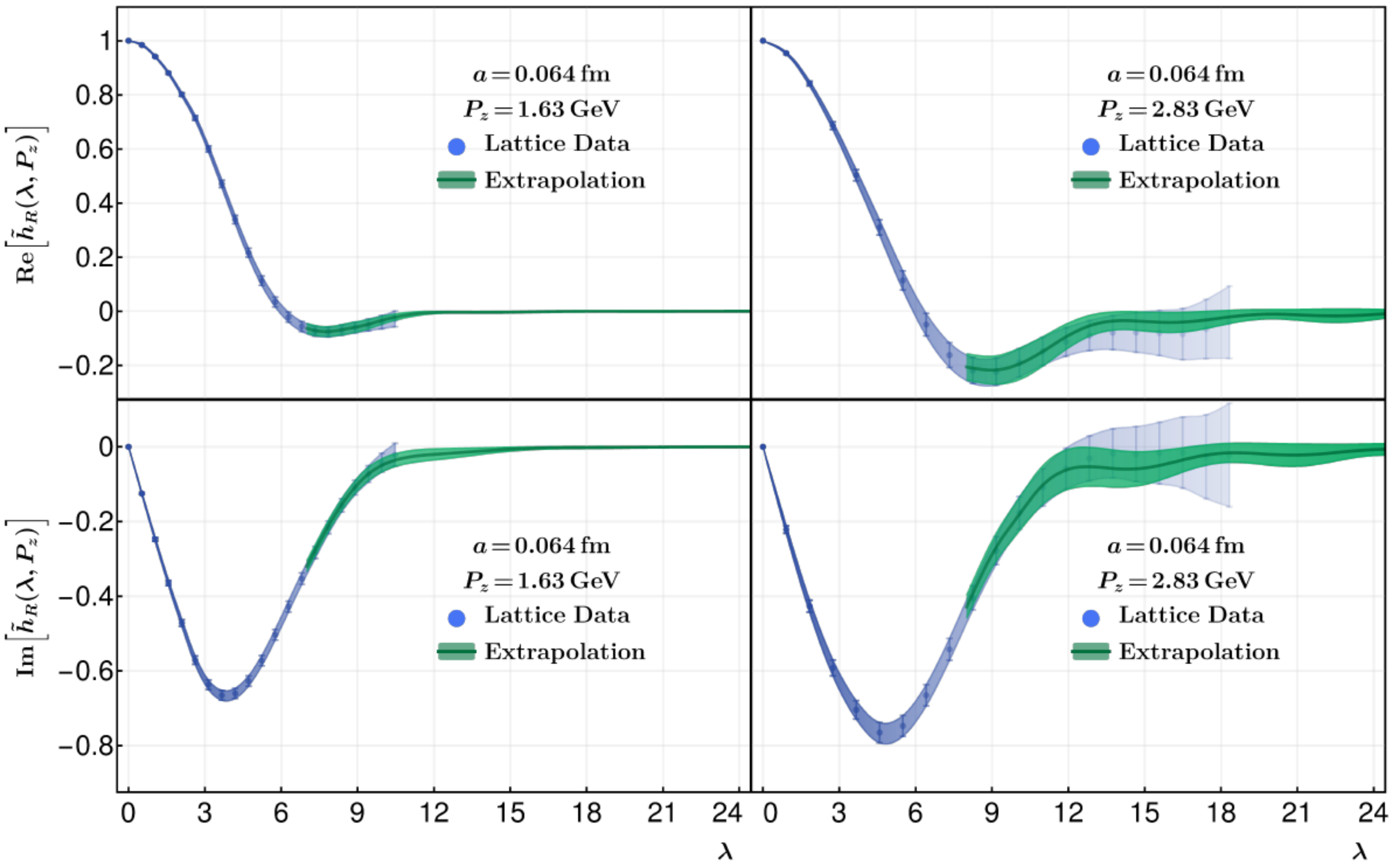

Figure 5: Renormalized matrix elements $\tilde{h}_\mathrm{R}(\lambda, P_z)$ for N203 for one small (left) and large (right) momentum with extrapolation to large λ. The extrapolation reproduces the data in moderate λ region and yields smooth correlations in large λ region.

- $\lambda \geq 7$ chosen for the extrapolation
- λ varied down to $\lambda \geq 4$ to estimate the systematic error from extrapolation

Backup slides: One-loop matching

- Calculation done in Feynman gauge

Coordinate space

- Consider transversity quasi-LF correlation with on-shell and massless external quark state

$$\tilde{h}(z, p_z, \mu) = \langle p|\bar{\psi}(z)\gamma^t\gamma^x\gamma^5 W[z,0]\psi(0)|p\rangle$$

  – $p^\mu = (p_0, 0,0, p_z)$: quark momentum

- Factorization in coordinate space:

$$\tilde{h}(z, \lambda = zp_z, \mu) = \int_0^1 d\alpha Z\left(\alpha, z^2, \mu^2\right) h(\alpha\lambda, \mu) + \mathrm{h.t.}$$

  – h.t.: higher-twist terms

  – Matching kernel in $\overline{\mathrm{MS}}$ scheme at one-loop level:

$$Z\left(\alpha, z^2\mu^2\right) = \delta(1-\alpha) + \frac{\alpha_s C_F}{2\pi}\left\{-\left(\frac{2\alpha}{1-\alpha}\right)_+ \left(\ln\frac{z^2\mu^2 e^{2\gamma_E}}{4} + 1\right) - \left(\frac{4\ln(1-\alpha)}{1-\alpha}\right)_+\right\}\theta(\alpha)\theta(1-\alpha)$$
$$+ \frac{\alpha_s C_F}{2\pi}\left(2\ln\frac{z^2\mu^2 e^{2\gamma_E}}{4} + 2\right)\delta(1-\alpha)$$

Backup slides: One-loop matching

- Begin with ratio scheme to obtain one-loop matching in the hybrid scheme

- Quasi-LF correlation at zero momentum and short distance given by

$$Z_0(z,\mu) = 1 + \frac{\alpha_S C_F}{2\pi}\left(2\ln\frac{z^2\mu^2 e^{2\gamma_E}}{4} + 2\right)$$

- Thus, one-loop matching in ratio scheme:

$$\boxed{Z_r(\alpha, z^2\mu^2) = \delta(1-\alpha) + \frac{\alpha_s C_F}{2\pi}\left\{-\left(\frac{2\alpha}{1-\alpha}\right)_+\left(\ln\frac{z^2\mu^2 e^{2\gamma_E}}{4} + 1\right) - \left(\frac{4\ln(1-\alpha)}{1-\alpha}\right)_+\right\}\theta(\alpha)\theta(1-\alpha)}$$

- From this, obtain one-loop matching kernel in hybrid scheme:

$$\boxed{Z_h\left(\alpha, z^2\mu^2, \frac{z^2}{z_s^2}\right) = Z_r(\alpha, z^2\mu^2) + \frac{\alpha_s C_F}{\pi}\ln\left(\frac{z^2}{z_s^2}\right)\delta(1-\alpha)\theta(|z| - z_s)}$$

  - Reduces to ratio scheme matching when $z_s \to \infty$

Backup slides: One-loop matching

Momentum space

- Transversity quasi-PDF defined as a Fourier transform of the quasi-LF correlation

$$\delta\tilde{q}\left(x, \frac{\mu}{p_z}\right) = \int_{-\infty}^{\infty} \frac{d\lambda}{2\pi}\, e^{ix\lambda} \tilde{h}\left(\lambda, \frac{\mu^2\lambda^2}{p_z^2}\right)$$

- Thus, matching kernel in momentum space related to that in coordinate space by double FT:

$$C\left(x, \frac{\mu}{p_z}\right) = \int_{-\infty}^{\infty} \frac{d\lambda}{2\pi} e^{ix\lambda} \int_{-1}^{1} d\alpha e^{-i\alpha\lambda} Z(\alpha, \frac{\mu^2\lambda^2}{p_z^2})$$

- Using this and the factorization formula, gives the result in ratio scheme

$$C_r\left(x, \frac{\mu}{p_z}\right) = \delta(1-x) + \frac{\alpha_s C_F}{2\pi} \begin{cases} [\frac{2x}{1-x} \ln\frac{x}{x-1} - \frac{2}{1-x}]_+ & x > 1 \\ \left[\frac{2x}{1-x}\left(\ln\frac{4p_z^2}{\mu^2} + \ln x(1-x)\right) + 2\right]_+ & 0 < x < 1 \\ [-\frac{2x}{1-x} \ln\frac{x}{x-1} + \frac{2}{1-x}]_+ & x < 0 \end{cases}$$

and hybrid scheme

$$C_h\left(x, \frac{\mu}{p_z}, \lambda_s\right) = C_r\left(x, \frac{\mu}{p_z}\right) + \delta C\left(x, \frac{\mu}{p_z}, \lambda_s\right) = C_r\left(x, \frac{\mu}{p_z}\right) + \frac{\alpha_s C_F}{\pi}\left[-\frac{1}{|1-x|} + \frac{2\mathrm{Si}\big((1-x)\lambda_s\big)}{\pi(1-x)}\right]_+$$

Backup slides: Dependence of momentum space distribution on m_π

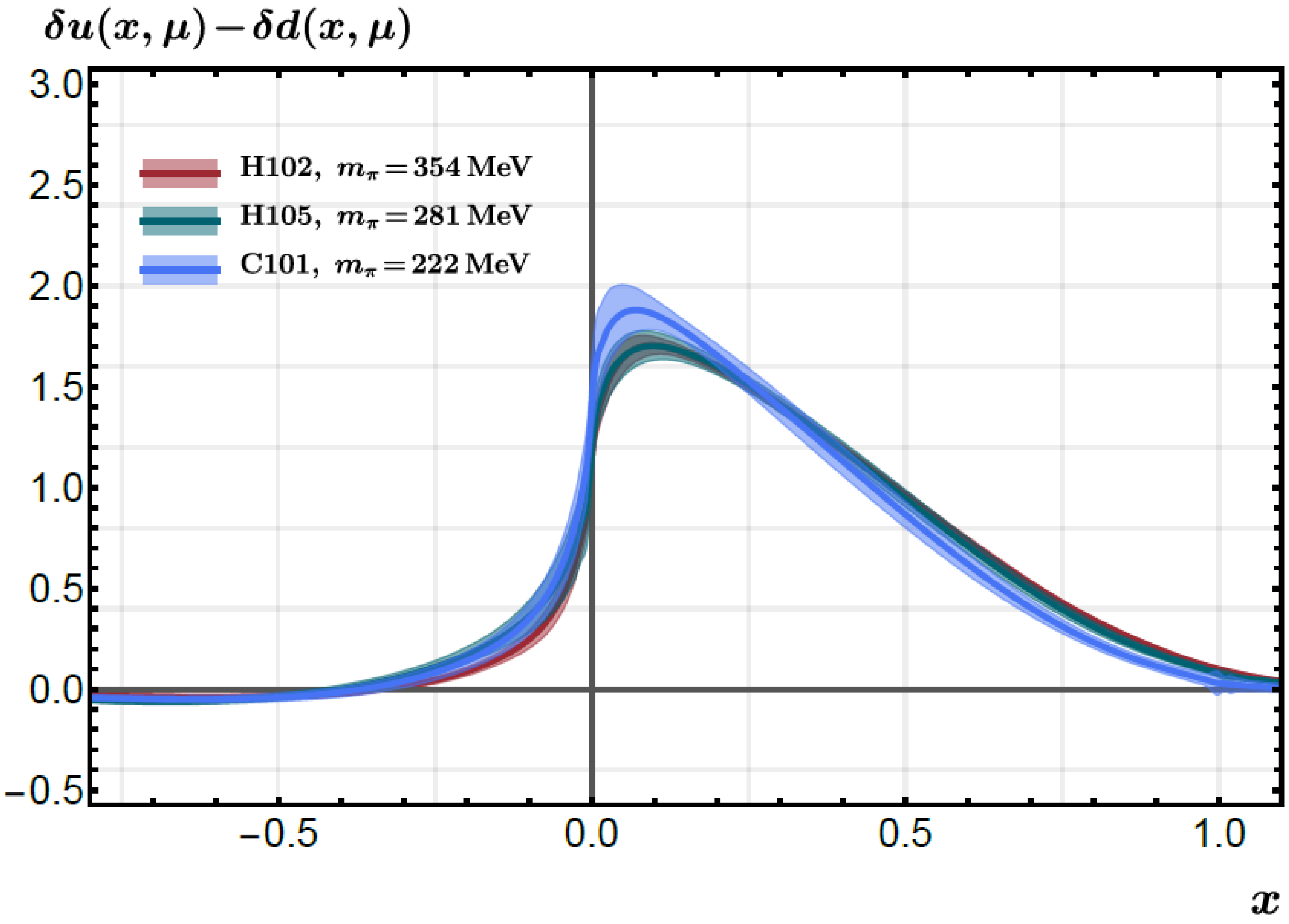

The pion mass dependence of the extracted PDF on different ensembles with the same lattice spacing $a = 0.085$ fm and nucleon momentum $P_z = 1.82$ GeV. Only statistical errors.

- Pion mass dependence after NLO matching
- Only very small pion mass dependence

Backup slides: Dependence of momentum space distribution on P_z

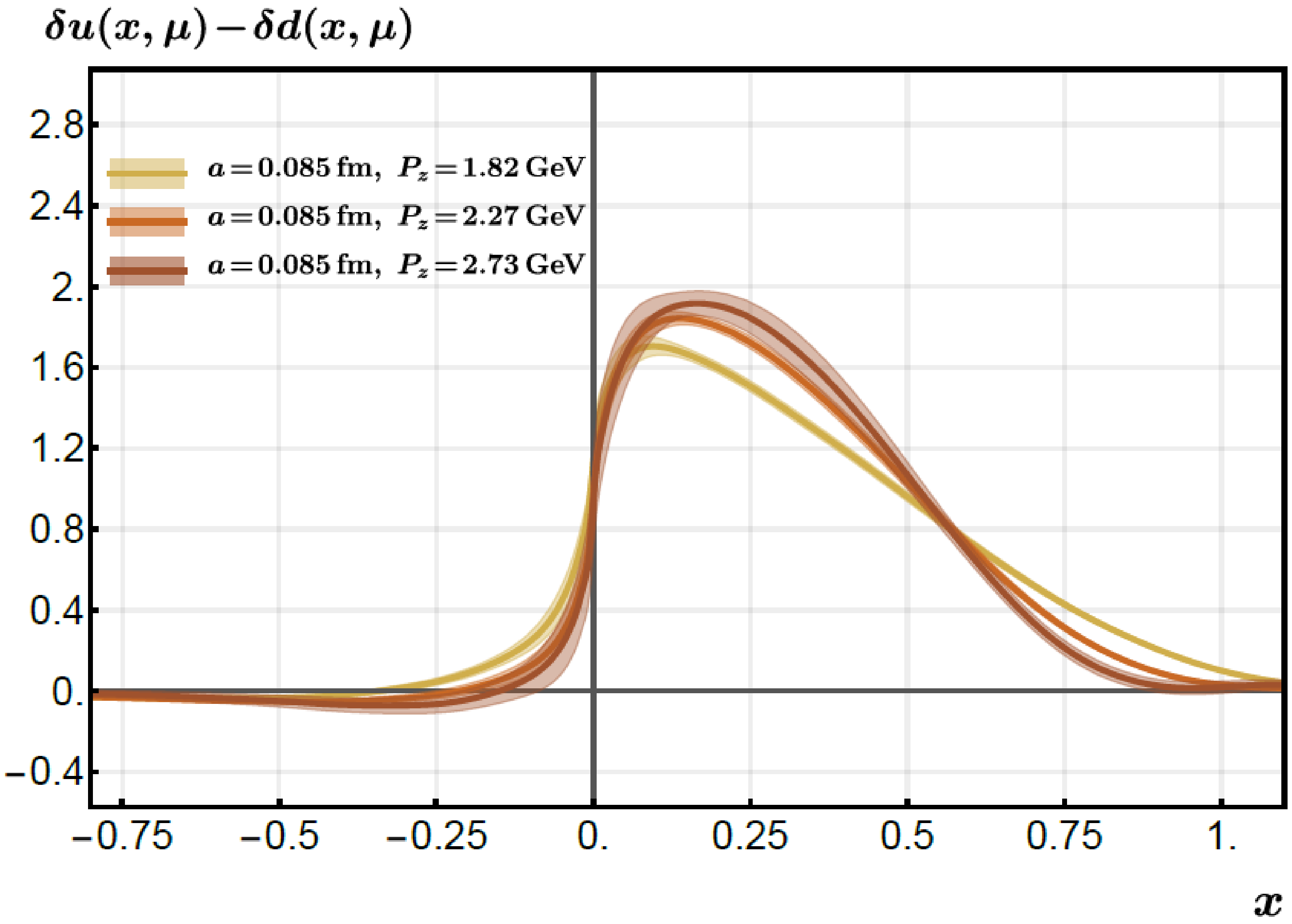

The momentum dependence of the extracted PDF on H102. Only statistical errors.

Backup slides: Dependence of momentum space distribution on a

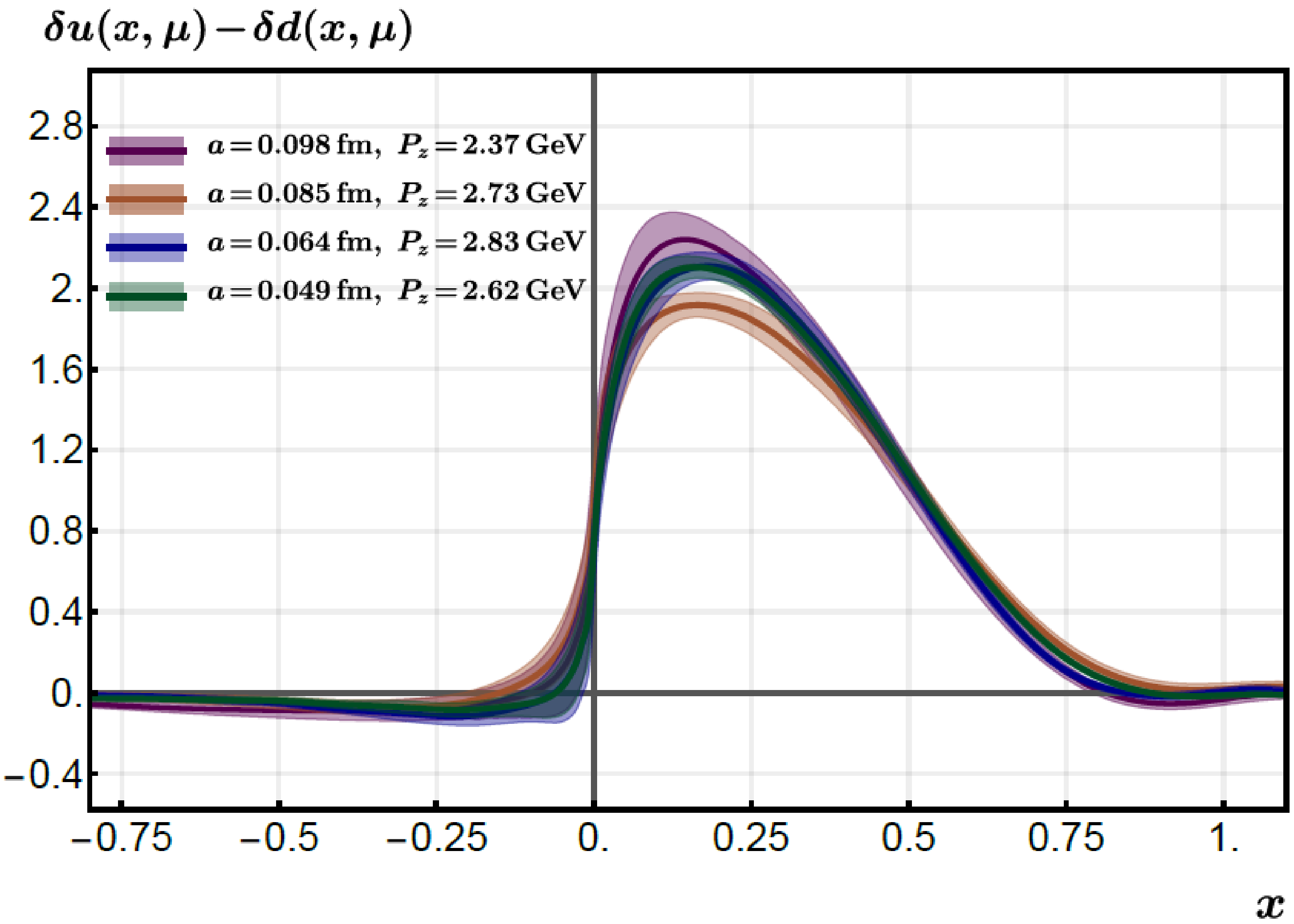

The a-dependence of the extracted PDF for different ensembles. Only statistical errors.

- Difficult to have the same momentum across different ensembles
- Illustrate a-dependence by plotting the PDFs obtained using the largest available momentum for each ensemble
- Good convergence
- X650 data shows large discretization artifacts, which is reflected in large errors (systematic uncertainties not even included here!) → very coarse lattices could be problematic for LaMET applications

Backup slides: Antiquark transversity

- Transversity at negative x can be interpreted as the antiquark transversity via the relation

$$\delta\bar{q}(x,\mu) = -\bar{q}(-x,\mu)$$

Backup slides: Sequential source method

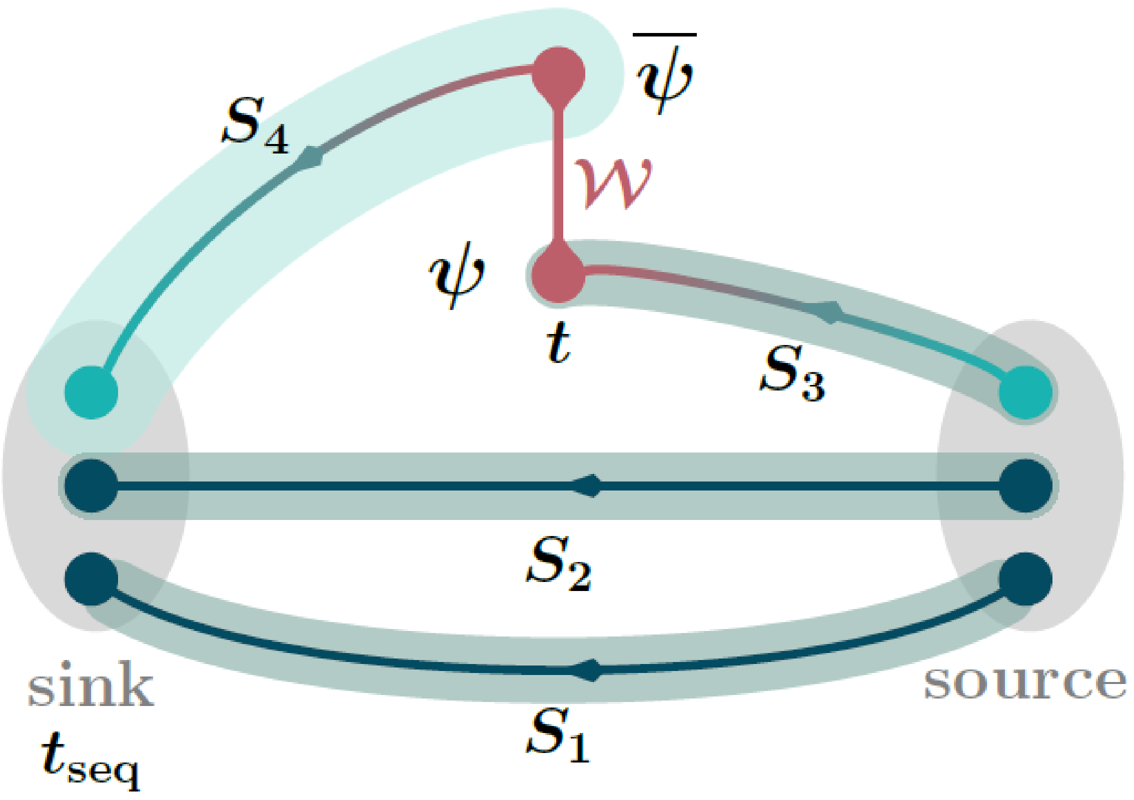

Illustration of the sequential source method. The time direction is from source to sink. Propagators $S_{1,2}$ are combined to construct the sequential source. The inversion with sequential source gives propagator S_4. S_4, S_3, gauge link W and necessary projectors are assembled to get the three-point correlator.

- Sequential source method with fixed sink to calculate the quark three-point correlator

Backup slides: Quasi light-cone distance λ

[2004.03543]

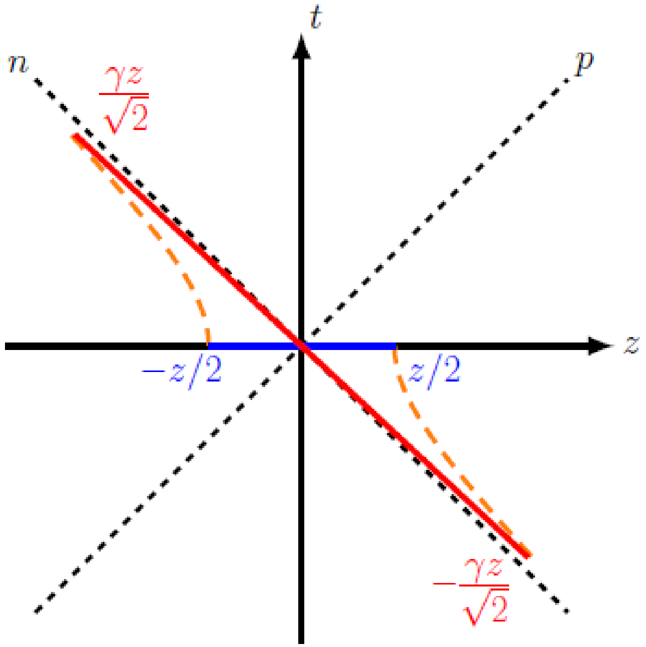

FIG. 6: The line segment in the z-direction in the frame of a large-momentum hadron. Through Lorentz boost, it is equivalent to a line segment of length $\sim \gamma z$ close to the light-one in the hadron state of zero momentum. Here $\gamma z/\sqrt{2}$ is the length of projection of the boosted line segment to the light-cone direction n. Thus, we call the dimensionless variable $\lambda = zP^z \sim \gamma z M$ as the quasi light-cone distance.

$\gamma = P^z/M$: boost factor

Backup slides: Systematic uncertainties

- **Renormalization scale dependence**
  - Estimated by varying the scale from 2 GeV to 3 GeV
  - Dominant systematic error in region $x > 0.2$
- **Choice of z_s in hybrid renormalization scheme**
  - Chose $z_s = 0.3$ fm, varied down to $z_s = 0.18$ fm → difference as systematic error
- **Extrapolation to large λ**
  - Different regions for extrapolation chosen to estimate the error
  - Mainly affects the small-x region $-0.2 < x < 0.2$
- **Combined extrapolation to continuum, infinite momentum and physical mass**
  - Error is relatively small